Neoplasma 2024; 71(3): 243–254

doi:10.4149/neo_2024_240108N8

Allicin inhibits the growth of HONE-1 and HNE1 human nasopharyngeal carcinoma cells by inducing ferroptosis

Xin LI#, Jin-Que LUO#, Xue-Qi LIAO, Shuo ZHANG, Li-Fan YANG, Tao WU, Ling WANG, Qing XU, Bin-Sheng HE, Zhen GUO*

Hunan Provincial Key Laboratory of the Research and Development of Novel Pharmaceutical Preparations, "The 14th Five-Year Plan" Application Characteristic Discipline of Hunan Province (Pharmaceutical Science), College of Pharmacy, Changsha Medical University, Changsha, Hunan, China

**Correspondence: plws3298@163.com*
#Contributed equally to this work.

Received January 8, 2024 / Accepted May 30, 2024

Allicin (AL) is one of garlic-derived organosulfides and has a variety of pharmacological effects. Studies have reported that AL has notable inhibitory effects on liver cancer, gastric cancer, breast cancer, and other cancers. However, there are no relevant reports about its role in human nasopharyngeal carcinoma. Ferroptosis is an iron-dependent form of non-apoptotic regulated cell death. Increasing evidence indicates that induction of ferroptosis can inhibit the proliferation, migration, invasion, and survival of various cancer cells, which act as a tumor suppressor in cancer. In this study, we confirmed that AL can inhibit cell proliferation, migration, invasion, and survival in human nasopharyngeal carcinoma cells. Our finding shows that AL can induce the ferroptosis axis by decreasing the level of GSH and GPX4 and promoting the induction of toxic LPO and ROS. AL-mediated cytotoxicity in human nasopharyngeal carcinoma cells is dependent on ferroptosis. Therefore, AL has good anti-cancer properties and is expected to be a potential drug for the treatment of nasopharyngeal carcinoma.

Key words: allicin; nasopharyngeal carcinoma; ferroptosis

Nasopharyngeal carcinoma (NPC) is a malignant tumor originating from the epithelial cells of the nasopharynx [1, 2]. NPC is characterized by distinct geographical distribution, with significantly higher incidence rates in Southeast Asia and southern China compared to Western countries [3-5]. Recently, the treatment for NPC is mainly radiotherapy, or a combination of radiotherapy and platinum-based chemotherapy [6]. However, malignant NPC cells are characterized by strong proliferative, migratory, and invasive capacities [7, 8], which severely constrain the therapeutic effect and result in a poor prognosis [9]. In addition, clinical data suggest that platinum therapy has a variety of adverse reactions, including diarrhea, alopecia, and loss of appetite [10]. Therefore, more novel effective treatment strategies and anticancer drugs for NPC therapy are urgently required.

Traditional Chinese medicines have a variety of biological activities and reliability compared with chemical medicines [11, 12]. It gradually gets the research focus from the field of antineoplastic drugs and has a great application future in the anti-cancer area [13, 14]. The Chinese medicine monomer allicin (AL), a product of hydrolysis and oxidation of primary sulfur-containing compounds γ-glutamyl-S-alk(en)yl-L-cysteines [15], which is one of the most biologically active molecules extracted from garlic [16]. AL has been applied in the clinic for decades with its pharmacological effects of anti-inflammatory, anti-bacterial, cardiovascular protection, and immunoregulatory activity [17–19]. Previous studies have reported that AL has notable inhibitory effects on liver cancer [20, 21], gastric cancer [22], ovarian cancer [23], breast cancer [24], glioma [25], colon cancer [26], lung cancer [27], renal clear cell carcinoma [28], and pancreatic cancer [29]. However, the inhibitory role and regulation mechanism of AL on NPC are scarcely known.

The discovery of regulated cell death processes has facilitated advances in cancer therapy [30, 31]. Ferroptosis is an iron-dependent form of non-apoptotic regulated cell death accompanied by the excessive accumulation of lipid peroxides (LPO), the consumption of lipid droplets (LD), and the production of reactive oxygen species (ROS) [32, 33], and is highly effective in eliminating tumor cells. The induction of ferroptosis instead of apoptosis can reduce tumor immune invasion and cancer-acquired drug resistance [34,

35]. Furthermore, glutathione peroxidase 4 (GPX4), as a key regulator of ferroptosis [36, 37], uses the depletion of GSH to promote the induction of toxic LPO and the obvious inhibition of cancer cell proliferation [38, 39]. A growing number of small molecules and approved drugs have been reported to induce ferroptosis in cancer cells and inhibit the proliferation of tumor cells [40–42]. However, whether AL can inhibit the expression of GPX4 and result in the induction of ferroptosis in NPC is still unclear. Thus, in the present study, we aimed to explore the inhibitory role of AL on the proliferation, migration, and invasion of NPC cells as well as to elucidate whether the mechanism underlying the actions is involved in the ferroptosis pathway.

Materials and methods

Antibodies and reagents. Antibodies for β-actin (20536-1-AP) and GPX4 (ab125066) were purchased from Proteintech Group (Rosemont, USA) and Abcam (Cambridge, UK) respectively. Allicin (AL), α-tocopherol (α-Toc), and ferrostatin-1 (Fer-1) were obtained from Med Chem Express (NJ, USA). 2',7'-dichlorofluorescin Diacetate (DCFH-DA), a live/dead assay kit, Tetramethyl rhodamine Ethyl Ester (TMRE) dye, and radioimmunoprecipitation assay (RIPA) buffer were purchased from Beyotime Biotechnology Co., Ltd (Shanghai, China). BODIPY 581/591-C11 (no. 27086) and BODIPY 493/503 (no. 25892) were purchased from Cayman Chemical (MI, USA). A glutathione (GSH) assay kit and an EdU assay kit were purchased from Keygen Biotechnology Co., Ltd (Nan-jing, China). RPMI medium 1640, penicillin-streptomycin, fetal bovine serum (FBS), and Dulbecco's phosphate-buffered saline (PBS) were purchased from Thermo Fisher (MA, USA). Cell Counting Kit-8 (CCK-8) was purchased from Dojindo Laboratories (Tokyo, Japan).

Cell culture. The human NPC cell lines HONE-1 and HNE1 were obtained from the ATCC. HONE-1 and HNE1 cell lines were both derived from a poorly differentiated NPC biopsy specimen and lost the Epstein-Barr virus genome as cells were passaged [43]. These cell lines were cultured in RPMI medium 1640 supplemented with 10% FBS and 1% penicillin-streptomycin under a 37 °C humid atmosphere containing 5% CO_2. The authenticity of all cell lines was verified by short tandem repeat analysis within the last 3 years. All experiments were performed with mycoplasma-free cells.

Cell viability assay. The CCK-8 assay was applied to test the viability of HONE-1 and HNE1 cells as described in a previous study [44]. Cells (5×10^3/well) were seeded into a 96-well culture plate (Corning, NY, USA) for 24 h. Then cells were incubated with or without serial dilutions of AL for 24 h or 48 h and 72 h. Then the CCK-8 detection reagent was added and incubated for 2 h. The absorbance at 450 nm was measured by a microplate reader (Thermo Fisher Scientific, USA).

EdU staining. The EdU staining assay was applied to test cell proliferation of HONE-1 and HNE1 cells as previously reported [45]. Cells (5×10^3/well) were seeded into a 96-well culture plate (Corning, NY, USA) for 24 h. Then cells were incubated with AL (1.5 mM) for 24 h. Then the cell proliferation was examined using an EdU kit (Shanghai KeyGene Biotechnology Co., Ltd.) according to the manufacturer's instructions and quantified by the ImageJ software.

Plate colony formation assay. The colony formation assay was applied to test the colonies of HONE-1 and HNE1 cells according to the protocol as described in a previous study [46]. 500 viable cells were plated in a 6-well plate and cultured overnight. Fresh RPMI 1640 medium with or without AL (1.5 mM) was added to the plate and then cultured at 37 °C for 24 h. Then the medium was replaced with RPMI 1640 containing 10% FBS and 1% penicillin-streptomycin every 3 d for approximately 14 d. To visualize and count the colonies, we separately used 4% polyoxymethylene (Beijing Solarbio Biotechnology Co., Ltd., P8430) and 0.5% crystal violet (Beijing Solarbio Biotechnology Co., Ltd., G1061) to fix and stain the colonies. The colony numbers were quantified by the ImageJ software.

Western blot analysis. Cell extracts were prepared using RIPA lysis buffer containing phosphatase and protease inhibitors as previously reported [47]. Lysates were centrifuged at 12,000×g for 30 min at 4 °C, and the supernatant was collected. The concentration was determined by using a BCA protein quantitative kit (Jiangsu KeyGene Biotechnology Co., Ltd.). Concentration-normalized lysates were mixed with loading buffer and then boiled at 100 °C for 10 min. Proteins were separated by SDS-PAGE (80 V for 30 min and 120 V for 1 h) and transferred to PVDF membranes (400 mA for 45 min). The membranes were blocked with a Quick blocking solution (Shanghai Beyotime Biotechnology Co., Ltd.) for 15–20 min, followed by incubating with indicated primary antibodies (anti-β-actin and anti-GPX4) at 4 °C overnight. After washing with TBST, the membranes were incubated with secondary antibodies for 1–2 h at room temperature. After washing with TBST, the membranes were visualized by an Enhanced Chemiluminescence (ECL) Kit (Biosharp) according to the manufacturer's instructions. Images were captured with a Bio-Rad imaging system. The relative density of each blot was normalized to the corresponding β-actin levels using the ImageJ software.

Survival, migration, and invasion assay. For survival experiments, the live/dead assay was applied to test cell survival of HONE-1 and HNE1 cells. Cells (5×10^3/well) were seeded into a 96-well culture plate (Corning, NY, USA) for 24 h. Then cells were incubated with AL (1.5 mM) with or without ferrostatin-1 (Fer-1, 2 μM) or α-tocopherol (α-Toc, 25 μM) for 24 h. The cells were observed under a microscope. Then the cell survival was examined using a live/dead kit (Shanghai Beyotime Biotechnology Co., Ltd.)

according to the manufacturer's instructions and observed by an inverted fluorescent microscope (Olympus).

For migration and invasion experiments, the Transwell without and with Matrigel pre-coated filter membranes were employed respectively as previously reported [48, 49]. Both migration and invasion are two major features of cancer cells [50]. Migration refers to the ability of cells to move, while invasion is the ability of cells to move while secreting proteins that digest the extracellular matrix (ECM) and remove movement disorders [50]. So Transwell assay without Matrigel was used to detect the migration ability of cells, and the Transwell assay with Matrigel was used to detect the invasion ability of cells [51, 52]. HONE-1 and HNE1 cells (1×10^4 cells/well) were suspended in serum-free medium and plated into the upper chamber with or without AL (1 mM). In the lower chamber, 500 μl complete medium containing 10% FBS were added. After 24 h, cells on the reverse side of the upper chamber were fixed with 4% paraformaldehyde for 20 min, washed with PBS and stained with 0.5% crystal violet for 10 min. Finally, cells were washed with PBS and dried by air. Cells that had migrated and invaded through the filter membranes were observed by a microscope (100× Olympus).

Lipid peroxidation measurement. The intracellular lipid peroxidation levels were measured with C11-BODIPY (581/591). C11-BODIPY (581/591) is a fluorescent radioprobe for indexing lipid peroxidation in living cells [53]. Briefly, the HONE-1 and HNE1 cells were incubated with AL (1.5 mM) with or without ferrostatin-1 (Fer-1, 2 μM) or α-tocopherol (α-Toc, 25 μM) for 24 h. Then serum-free medium containing 5 μM C11-BODIPY (581/591) was added into the cells and incubated for 20 min. Finally, the fluorescence intensity was then measured with an inverted fluorescent microscope (Olympus) and quantified by the ImageJ software.

Lipid droplets assay. The intracellular lipid droplet levels were measured with BODIPY 493/503. BODIPY (493/503) is a cell permeable lipophilic fluorescence dye emitting green fluorescence and it stains neutral LD in live or fixed cells [54]. Briefly, the HONE-1 and HNE1 cells were incubated with AL (1.5 mM) with or without ferrostatin-1 (Fer-1, 2 μM) or α-tocopherol (α-Toc, 25 μM) for 24 h. Then the cells were fixed with 4% paraformaldehyde for 15 min at room temperature and then stained with BODIPY 493/503 working solution (2 μM) for 15 min at 37 °C. After washing with PBS, cells were subjected to an inverted fluorescent microscope (Olympus) observation and quantified by the ImageJ software.

***In vitro* ROS study.** Briefly, the HONE-1 and HNE1 cells were incubated with AL (1.5 mM) with or without ferrostatin-1 (Fer-1, 2 μM) or α-tocopherol (α-Toc, 25 μM) for 24 h. DCFH-DA (10 μM) was incubated with the HONE-1 and HNE1 cells for 30 min. After washing, the cells were observed by an inverted fluorescent microscope and quantified by the ImageJ software. Because non-fluorescent DCFH-DA could be oxidized to fluorescent DCF by ROS, the fluorescence change indicated the generation of ROS.

***In vitro* GSH study.** The HONE-1 and HNE1 cells were seeded in 6-well plates and incubated overnight. After treating with AL (1.5 mM) for 24 h, the GSH content of different groups was measured using a GSH Assay kit, and the absorbance was measured by a microplate reader (Thermo Fisher Scientific, USA). The relative content of GSH was acquired based on the comparison to the GSH content of untreated cells.

Transmission electron microscopy experiment. The morphology of cells treated with AL (1.5 mM) was observed by a transmission electron microscope (TEM, EM10CR, Zeiss, Imagery facility, Institut Cochin). The HONE-1 and HNE1 cells (about 5×10^5/well) were plated in a 6-well culture plate (Corning, NY, USA) and incubated overnight. Then AL was added into the 6-well culture plate and incubated for 24 h. The culture medium was poured off the cells and 2–3 ml of 2.5% glutaraldehyde fixative that had returned to room temperature was added. After the cells are fixed at room temperature in the dark for 5 min, they are quickly shoveled down in one direction with a cell scraper at an oblique angle of 45°. The obtained cell suspension was sucked into a centrifuge tube, centrifuged (1,500–3,000×g) for 3–5 min, and the supernatant was discarded. A new 2.5% glutaraldehyde fixative was then added. If the cells failed to agglomerate, about 5 μl of blood could be added. The clear mixture was centrifuged again until a dense cell mass appeared at the bottom of the tube. After fixation at room temperature in the dark for 30 min, the plates were stored at 4 °C. Finally, ultrathin sections were made and TEM was performed to visualize cell morphology changes.

Mitochondrial activity assay. Tetramethyl rhodamine ethyl ester (TMRE) dye was used to label the mitochondria of living cells [55]. When the mitochondrial structure was damaged, the red fluorescence of TMRE was weakened or even disappeared. The HONE-1 and HNE1 cells were seeded in 96-well plates and incubated overnight. Then the HONE-1 and HNE1 cells were treated with AL (1.5 mM) for 24 h and incubated in a serum-free medium containing TMRE (5 μg/ml) at 37 °C for 20 min. After washing with serum-free medium, cells were observed by an inverted fluorescent microscope (Olympus) and quantified by the ImageJ software.

Statistical analysis. The statistical analysis was performed using SPSS version 17.0. Quantitative data were representative of three independent replicates. One-way ANOVA was used for multiple comparisons between groups and a two-tailed independent t-test for a single comparison between two groups as described in a previous study [56]. Statistical tests are justified as appropriate, and the data meet the assumptions of the tests. All values are presented as the mean ± SEM. p-value <0.05 was considered statistically significant.

Results

Allicin inhibits the proliferation of human nasopharyngeal carcinoma cells. To explore the effect of AL on the proliferation of human NPC cells, we set up different concentrations by consulting the literature. The control group was DMSO. Two human NPC cell lines HONE-1 and HNE1 were treated with AL for 24 h, and then performed CCK-8 cell viability assay experiments. Compared to the control group, the cell viability showed a significant drop in 1.5 mM, 2 mM, and 2.5 mM AL-treated cells (Figure 1A). Thus, we choose the minimal effective concentration of 1.5 mM for the further experiment. The results showed that the cell viability was inhibited in a time-dependent manner after treatment with 1.5 mM AL (Figure 1B). To verify this result, we performed EdU incorporation experiments and plate colony formation experiments. The results of the EdU incorporation experiments showed that compared with the control group, the EdU-positive percentage of the cells in the treatment group was significantly decreased (Figures 1C, 1D). Plate colony formation experiments also showed that the cloning ability of NPC cells was obviously weakened after treatment with

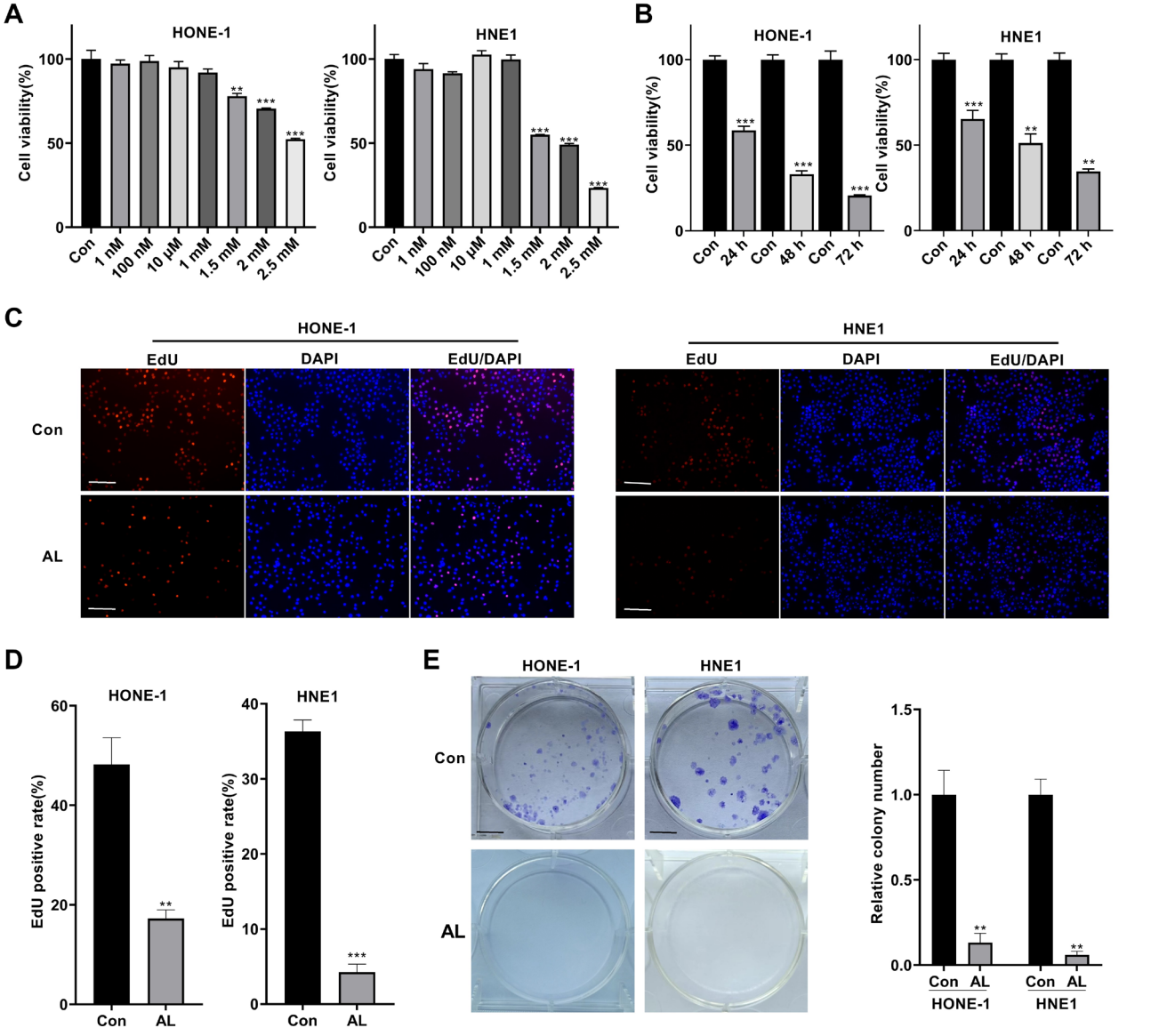

Figure 1. The cytotoxic effect of AL on HONE-1 and HNE1 cells. A) The cell viability of HONE-1 and HNE1 cells treated by AL with different concentrations was examined by the CCK-8 assay. B) The cell viability of HONE-1 and HNE1 cells treated by AL (1.5 mM) at different times was examined by the CCK-8 assay. C, D) EdU-positive HONE-1 and HNE1 cells treated by AL (1.5 mM) were examined by the EdU staining (C–D), scale bar = 200 μm. E) The colony formation of HONE-1 and HNE1 cells treated by AL (1.5 mM) was examined by the colony formation experiments (scale bar = 5 mm). **p<0.01; ***p<0.001 vs. Con. Error bars represent the standard error of the mean.

AL (Figure 1E). These results proved that AL significantly inhibited the growth and proliferation of NPC cells.

Allicin inhibits the migration and invasion of human nasopharyngeal carcinoma cells. NPC is a common and highly aggressive malignant tumor worldwide. Therefore, we explored the influence of AL on the migration and invasion of NPC cells. Cell migration is the movement of cells from one region to another in response to external signals such as chemokines. This process plays an important role in physiological and pathological aspects, such as injury repair, cell differentiation, malignant tumor metastasis, immune cell migration, tissue repair, and so on. Cell invasion is similar to cell migration, but cell invasion requires cells to move through the ECM layer, enzymatically removing the ECM barriers, and then moving from one place to another driven by a gradient of chemokine concentration. So, we conducted the Transwell experiments to verify the migration and invasion ability of NPC cells with and without Matrigel. The results showed that the migration ability of NPC cells after AL treatment for 24 h was significantly lower than that of the control group (Figures 2A, 2B). It indicated that AL obviously prevented the movement of NPC cells. Besides, the invasion ability of NPC cells after AL treatment for 24 h was also significantly lower than that of the control group (Figures 2C, 2D). It is demonstrated that AL effectively inhibited the ability of NPC cells to move after removing the ECM barriers. These results confirmed that AL significantly inhibited the migration and invasion of NPC cells.

Allicin inhibits the survival of human nasopharyngeal carcinoma cells. To investigate the effect of AL on the survival of human NPC cells, the HONE-1 and HNE1 cell lines were treated with AL for 24 h and then observed under a microscope. The results showed that the quantity and morphology of NPC cells changed obviously (Figures 3A, 3B). Then, we designed a live/dead assay to further detect whether AL has the ability to inhibit the survival of NPC cells *in vitro*. The results showed that compared with the control group, the live NPC cells were significantly reduced after AL treatment for 24 h (Figures 3C, 3D). These results confirmed that AL significantly inhibited the survival of NPC cells.

Allicin induces ferroptosis of human nasopharyngeal carcinoma cells. To test whether AL can induce ferroptosis of human NPC cells, we performed the biology TEM (Bio-TEM) experiments. The images showed evident shrinkage of mitochondrial volume and reduction of mitochondria crista in the AL-treated cells (Figure 4A), which were recognized as morphological features of ferroptosis [2, 35]. Furthermore, we used TMRE staining to further confirm the changes of mitochondria. The results showed that the red fluorescence of mitochondria in the AL-treated cells was reduced obviously compared with the control group (Figure 4B). It indicated that AL could significantly inhibit the mitochondria activity

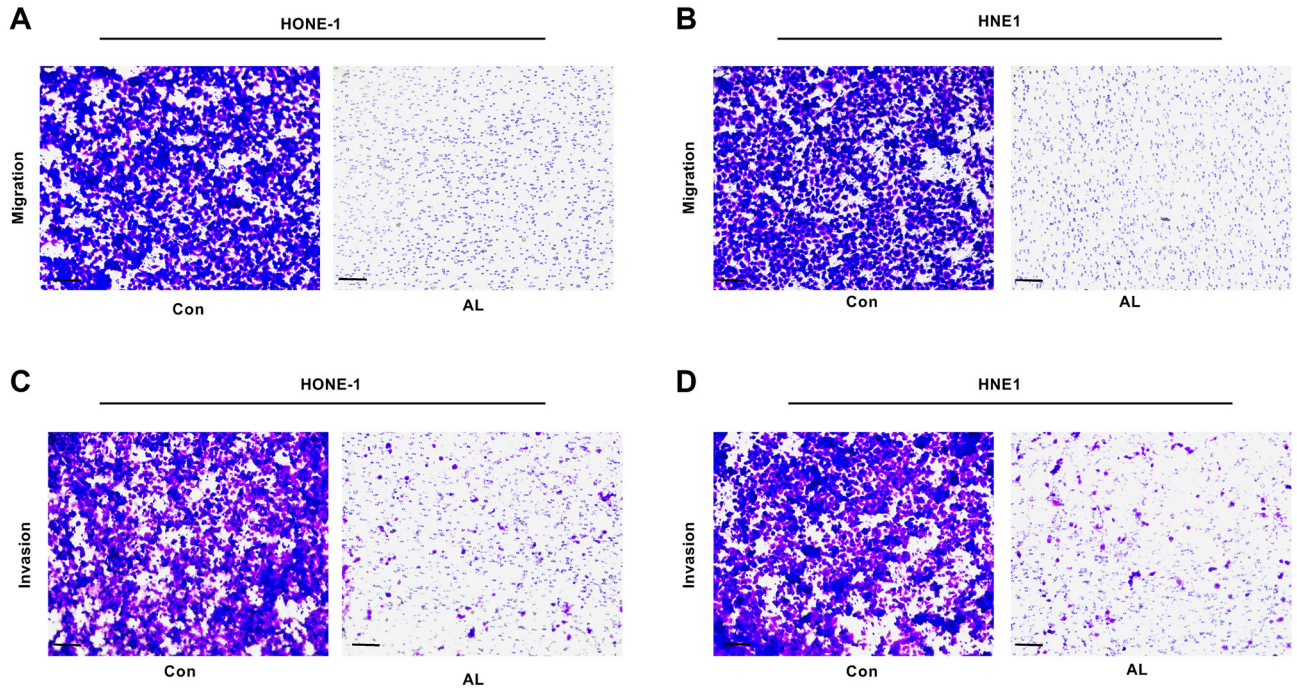

Figure 2. The effect of AL on migration and invasion of HONE-1 and HNE1 cells. A, B) The Transwell experiment without Matrigel detected the migration ability of HONE-1 and HNE1 cells treated with AL (1 mM). Cells that had migrated through the filter membranes were stained with 0.5% crystal violet for 10 min and observed by a microscope. C, D) The Transwell experiment with Matrigel detected the invasion ability of HONE-1 and HNE1 cells treated with AL (1 mM). Cells that had invaded through the filter membranes were stained with 0.5% crystal violet for 10 min and observed by a microscope (scale bar = 100 μm).

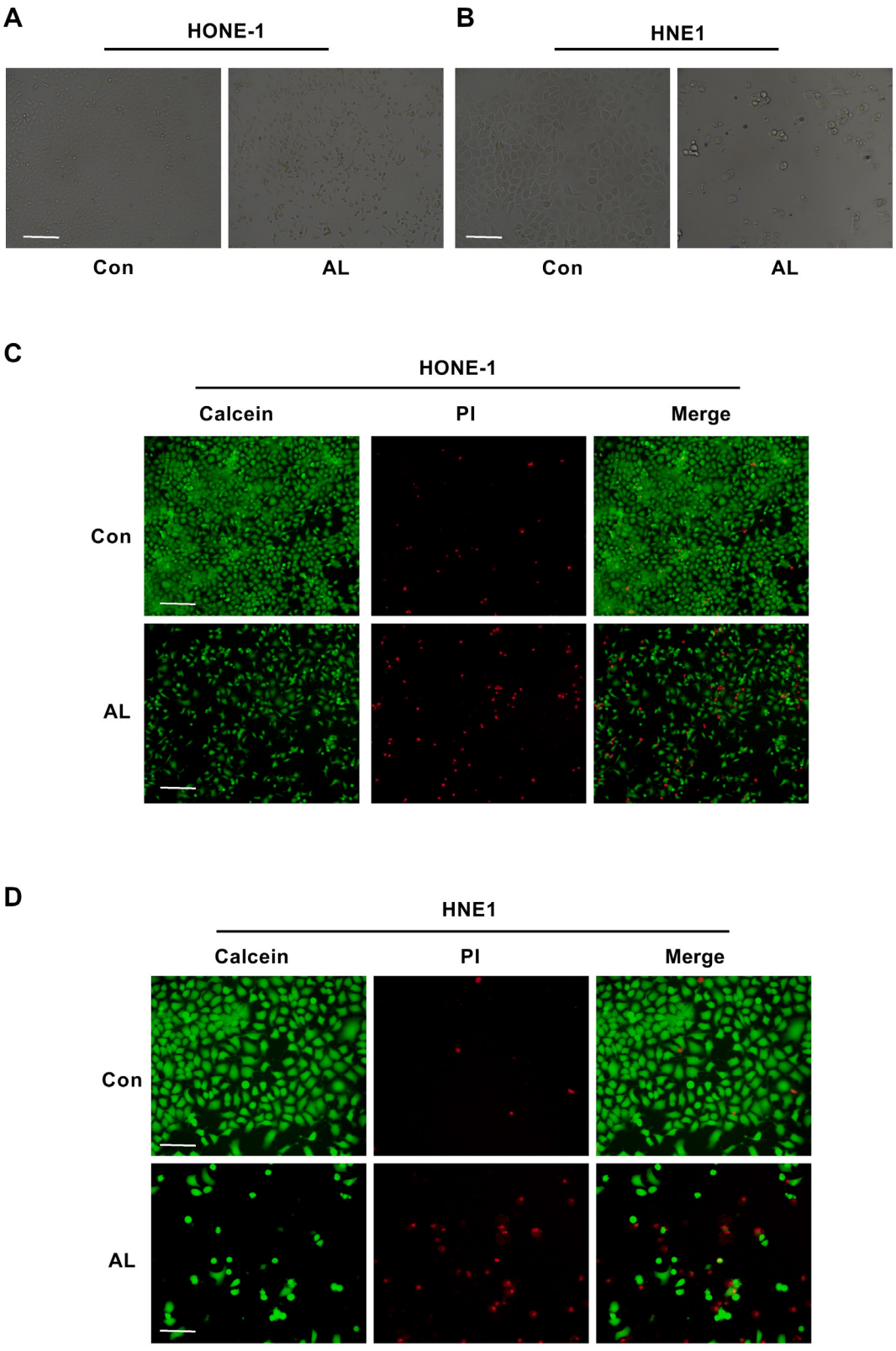

Figure 3. The effect of AL on survival of HONE-1 and HNE1 cells. A, B) Phenotypes of HONE-1 and HNE1 cells treated with AL (1.5 mM) were observed by a microscope. C, D) The survival of HONE-1 and HNE1 cells treated by AL (1.5 mM) were examined by a live/dead assay and observed by an inverted fluorescence microscopy (Calcein (green) = live cells, PI (red) = dead cells; scale bar = 100 μm).

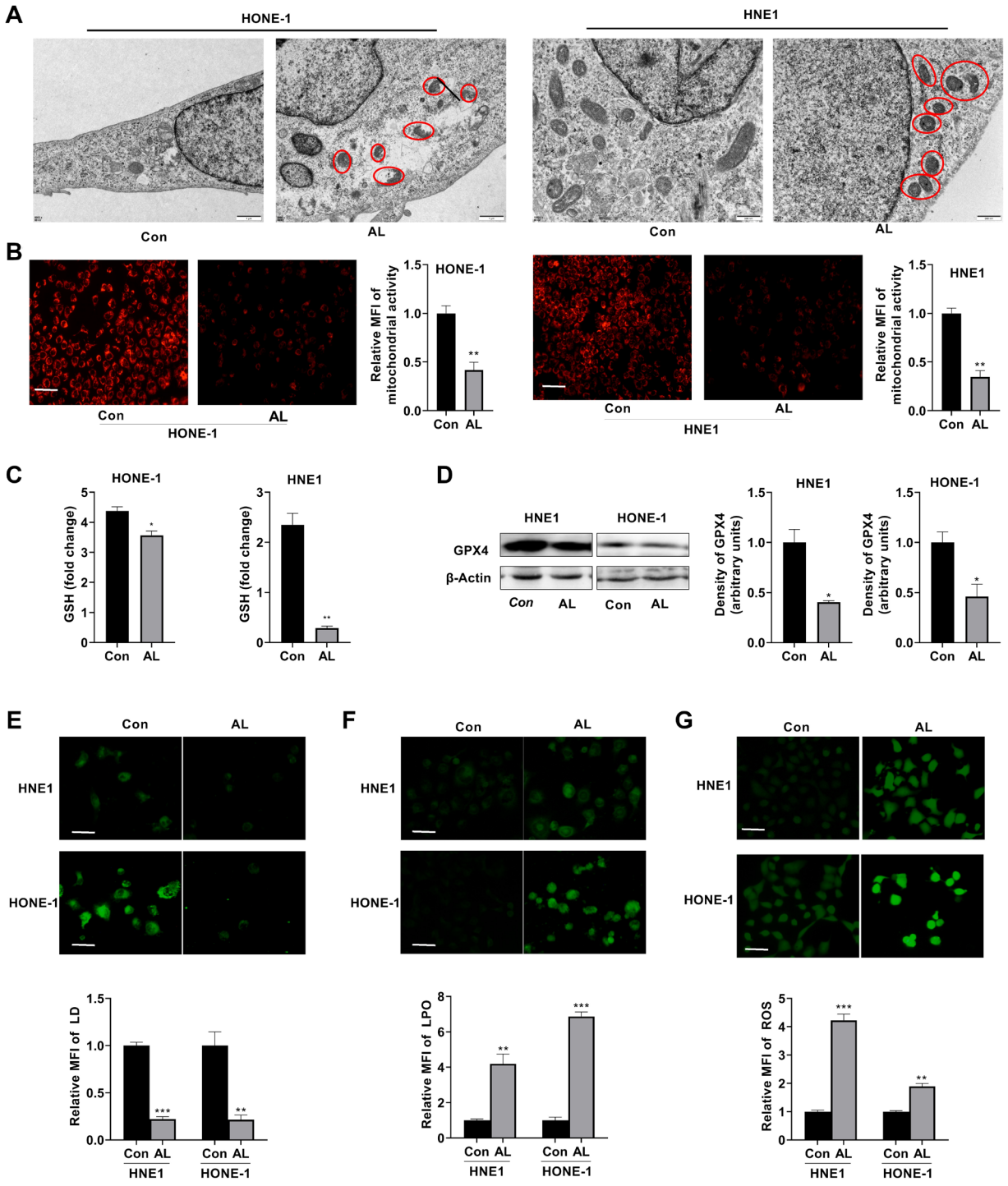

Figure 4. AL facilitated the lipid peroxidation and induced ferroptosis in HONE-1 and HNE1 cells. A) The images of HONE-1 and HNE1 cells treated by AL (1.5 mM) were examined by Bio-TEM experiments (scale bar = 100 μm). B) The mitochondrial staining images of HONE-1 and HNE1 cells treated by AL (1.5 mM) were examined by an inverted fluorescence microscopy (scale bar = 50 μm). C) The GSH level of HONE-1 and HNE1 cells treated by AL (1.5 mM) was assessed by GSH assay and examined by a microplate reader. D) The GPX4 levels of HONE-1 and HNE1 cells treated by AL (1.5 mM) were assessed by western blotting assay (antibodies: GPX4 and β-actin) using a Bio-Rad imaging system and the relative density of each blot was normalized to the corresponding β-actin levels. E) The LD level of HONE-1 and HNE1 cells treated by AL (1.5 mM) were stained with BODIPY 493/503 working solution (2 μM) and assessed by an inverted fluorescence microscope. F) The LPO level of HONE-1 and HNE1 cells treated by AL (1.5 mM) were stained with C11-BODIPY (581/591) working solution (5 μM) assessed by an inverted fluorescence microscope. G) The ROS level of HONE-1 and HNE1 cells treated by AL (1.5 mM) were stained with DCFH-DA working solution (10 μM) and assessed by an inverted fluorescence microscope (scale bar = 25 μm). *p<0.05; **p<0.01; ***p<0.001 vs. Con. Error bars represent the standard error of the mean.

of human NPC cells. In view of that GSH depletion, GPX4 downregulation, the consumption of LD, and the promotion of LPO and ROS are four crucial events during ferroptosis [36, 37], we further evaluated the changes of GSH, GPX4, LD, LPO, and ROS in AL-treated cells. As expected, our results showed that AL treatment obviously reduced cellular GSH level (Figure 4C). It suggested that the oxidative stress was increased in cells after AL treatment. GPX4 is a key negative regulator of ferroptosis. As shown in Figure 4D, AL significantly downregulated GPX4 expression in HONE-1 and HNE1 cells, promoting the occurrence of ferroptosis. LD could be used to combat oxidative stress damage and promote the survival of cancer cells, while ROS-induced LPO accumulation would destroy the function of normal cells and eventually promote the occurrence of ferroptosis. Finally, the results showed that AL treatment obviously decreased cellular LD levels, while increasing the levels of LPO and ROS (Figures 4E–4G). It implied that the cells lost the LD resistance to oxidative stress while accumulating large amounts of ROS and LPO accelerated the occurrence of ferroptosis. Together, all these results clearly indicated that AL could induce ferroptosis in human NPC cells.

Allicin-mediated cytotoxicity in human nasopharyngeal carcinoma cells is dependent on ferroptosis. To further investigate the effect of AL on ferroptosis, we assessed the effects of AL on the survival, LPO, ROS, and LD of HONE-1 and HNE1 cells in the presence and absence of ferrostatin-1 (Fer-1, a ferroptosis inhibitor) or α-tocopherol (α-Toc, one type of vitamin E that can eliminate LPO). Interestingly, in comparison with the cytotoxic effect of AL alone, co-treatment of Fer-1 or α-Toc significantly alleviated the cytotoxic effect of AL in HONE-1 and HNE1 cells (Figures 5A, 5B). Notably, Fer-1 or α-Toc observably reversed the accumulation of intracellular LPO and ROS induced by AL (Figures 5C, 5D). Moreover, Fer-1 or α-Toc also inhibited the reduction of LD induced by AL (Figure 5E). Taken together, these data demonstrated that AL was indeed capable of inducing ferroptotic cell death in human NPC cells.

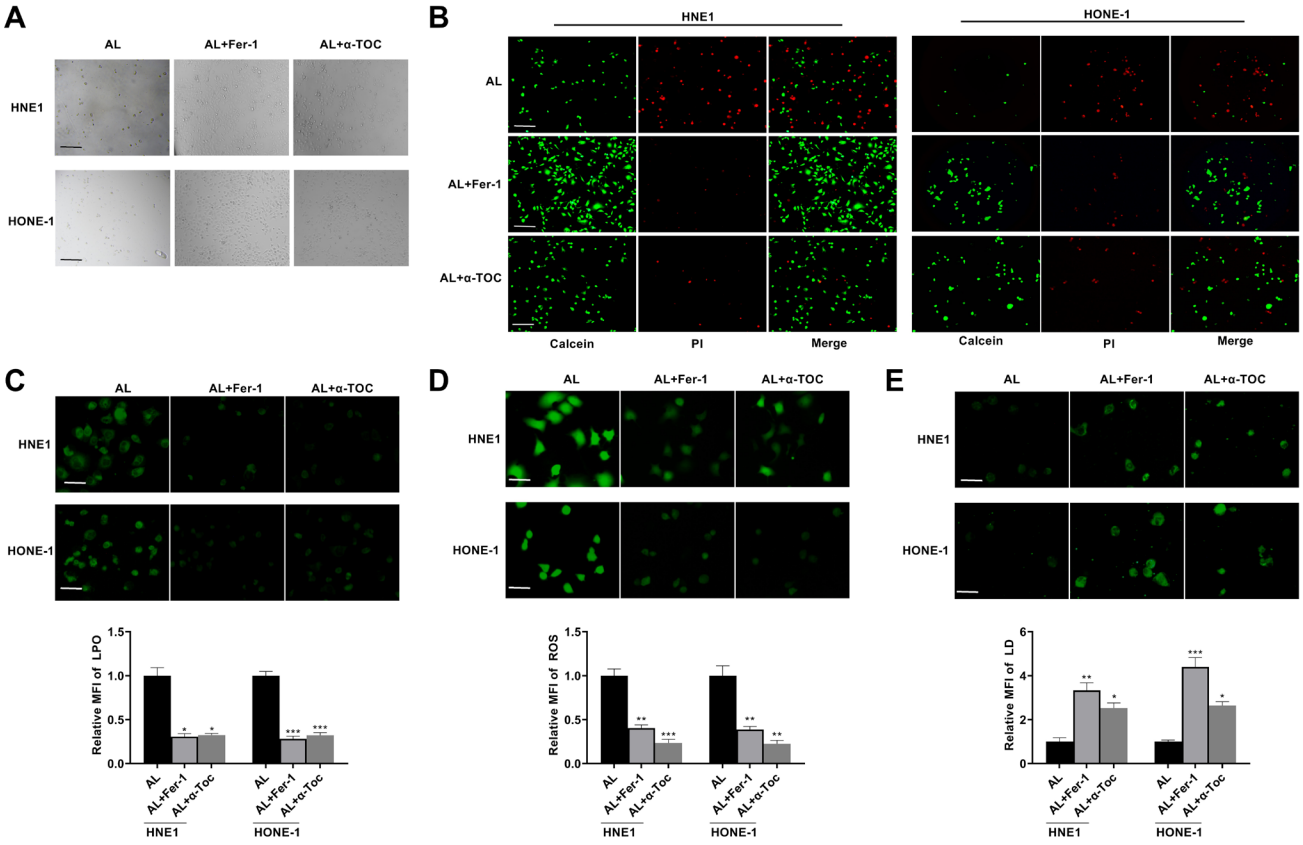

Figure 5. Inhibition of ferroptosis decreased the cytotoxicity of AL in HONE-1 and HNE1 cells. A) The phenotypes of AL-treated HONE-1 and HNE1 cells co-treatment with and without ferrostatin-1 (Fer-1, 2 μM) or α-tocopherol (α-Toc, 25 μM) were examined by a microscope (scale bar = 100 μm). B) The survival of AL-treated HONE-1 and HNE1 cells co-treatment with and without Fer-1 (2 μM) or α-Toc (25 μM) were examined by an inverted fluorescence microscopy (Calcein (green) = live cells, PI (red) = dead cells; scale bar = 100 μm). C) The LPO level of AL-treated HONE-1 and HNE1 cells co-treatment with Fer-1 (2 μM) or α-Toc (25 μM) were examined by an inverted fluorescence microscope (scale bar = 25 μm). D) The ROS level of AL-treated HONE-1 and HNE1 cells co-treatment with Fer-1 (2 μM) or α-Toc (25 μM) were examined by an inverted fluorescence microscope (scale bar = 25 μm). E) The LD level of AL-treated HONE-1 and HNE1 cells co-treatment with Fer-1 (2 μM) or α-Toc (25 μM) were examined by an inverted fluorescence microscope (scale bar = 25 μm). *p<0.05; **p<0.01; ***p<0.001 vs. AL. Error bars represent the standard error of the mean.

Discussion

The malignant proliferation of cancer cells is conducive to the occurrence and development of tumors [7, 57]. To achieve cancer treatment by inhibiting the proliferation of cancer cells by drugs is impressive [58, 59]. AL has potential anti-tumor activities, one of which involves cell proliferation. A large number of previous investigations reported that AL could inhibit the proliferation of various cancer cells. In oral tongue squamous cell carcinoma, AL was reported to repress cancer cell proliferation via induction of cell apoptosis [16]. In glioma, AL effectively inhibited the U87 glioma cell proliferation through an ERK-dependent pathway or by reducing IFN-β and IL-6 [25, 60]. In lung cancer, AL significantly decreased the A549 cell proliferation in both hypoxia and normoxia via autophagy and apoptosis pathways [61]. In neuroblastoma, AL inhibited human neuroblastoma cell proliferation by repressing ornithine decarboxylase enzyme activity [62]. In cholangiocarcinoma, AL obviously suppressed the cholangiocarcinoma cell proliferation by reducing the STAT3 signaling activation [63]. In ovarian cancer, AL affected the human ovarian cancer SKOV3 cell proliferation by mitochondrial Bax translocation and JNK activation [28]. In gastric cancer, AL inhibited the gastric cancer cell MGC-803 proliferation via the p38 MAPK/caspase-3 pathway [22]. In our study, we demonstrated that AL significantly inhibited the proliferation of human NPC cells in the time and concentration-dependent manners. In our experiment, we chose a relatively wide concentration range of the tested substances, which is not a problem for all natural substances. In fact, as for the achievable concentration of AL in plasma in humans or in laboratory animal models, it is worth further exploration for applying AL for the anti-tumor effect and safety *in vivo*. In the nude mice models of cholangiocarcinoma, AL at 10 and 20 mg/kg doses was administered daily for four weeks [63]. In the mouse model of colorectal cancer, AL at 48 mg/kg dose was administered to achieve 5 g/day [64]. In the nude mice models of liver cancer, AL at 5 mg/kg/day dose was administered every 2 days for three weeks [20]. In the nude mice model of pancreatic cancer, AL at 10 mg/kg dose was administered weekly for four weeks [28]. All of these demonstrated the efficacy and safety of AL *in vivo*. It has been reported in the literature that there is a certain difference in the concentration of the drug between the *in vivo* model and the *in vitro* model. It is suggested that the concentration selection of natural substances should be considered more comprehensively in the *in vivo* model.

Furthermore, migration and invasion are also very important for cancer cells, especially for the poor prognosis of patients, which is very related to the metastasis of cancer cells [65, 66]. The metastasis of cancer cells depends on the migration and invasion ability of cancer cells. Therefore, inhibiting the migration and invasion of cancer cells is also a necessary means to achieve cancer therapy. Some drugs can only affect the proliferation of cancer cells, and some drugs can only affect the migration and invasion of cancer cells, which will limit their efficacy and thus affect their clinical application. In addition to inhibiting cancer cell proliferation, AL has also been reported to affect the migration and invasion of some cancer cells. AL obviously suppressed the migration and invasion in cholangiocarcinoma cells, cervical cancer cells, and gastric cancer cells [63, 67, 68]. Although it has been shown that some cancer cells are only regulated by AL for proliferation or migration and invasion, we demonstrated that AL can also affect the migration and invasion of NPC cells at concentrations that do not affect their proliferation.

It is obvious that drugs that only inhibit the proliferation, migration, and invasion of cancer cells can only curb the occurrence and development of tumors, and that drugs that directly kill cancer cells can achieve better results in cancer therapy. It is interesting to investigate whether AL can directly induce tumor cell death in addition to its effects on proliferation, migration, and invasion. In our study, we proved that AL significantly induced cell death of NPC cells. It is well known that tumor cell death takes many forms. Apoptosis is the most common form of cancer cell death induced by anticancer drugs [69]. In fact, a large number of studies reported that AL could induce apoptosis of various tumor cells, such as gastric cancer cells [70–72], glioma cells [25, 73], and ovarian cancer cells [23, 28]. Ferroptosis is a new form of cell death [74, 75]. Many drugs can induce cell death through the apoptosis pathway, which is easy to form drug resistance, but cannot induce cancer cell death through the ferroptosis pathway. It is worth verifying that whether AL has the potential to act as an inducer of ferroptosis in cancer cells. Therefore, we verified whether AL could induce ferroptosis in NPC. Interestingly, we demonstrated that AL obviously induced ferroptosis in human NPC HONE-1 and HNE1 cells. Furthermore, we found that AL-induced ferroptosis in NPC cells was dependent on LPO and ROS. We used LPO and ROS inhibitor to reverse the ferroptosis index and found that AL-induced ferroptosis in NPC cells could be reversed by these inhibitors.

In conclusion, AL could significantly inhibit the proliferation, migration, and invasion of human NPC HONE-1 and HNE1 cells. Furthermore, AL could induce cell death of human NPC HONE-1 and HNE1 cells through the ferroptosis pathway. It indicated that AL could be used as a ferroptosis inducer in the treatment of NPC, which provides a new idea for the therapy of NPC.

Acknowledgments: This work was supported by the National Natural Science Foundation of China (No. 82203235, No. 82104309), the Science Project of the Education Department of Hunan Province (Grant No. 22B0898), the Hunan Provincial Natural Science Foundation of China (No. 2024JJ6094, No. 2023JJ20042, No. 2021JJ40643), ESI Discipline Special Project of Changsha Medi-

cal University (No. 2022CYY010), The Science and Technology Innovation Program of Hunan Province (No. 2023RC3194), Changsha Outstanding Innovative Youth Training Plan (No. kq2209024), Training Plan for Young Backbone Teachers in Hunan Province (No. 2022214).

References

[1] CHEN YP, CHAN ATC, LE QT, BLANCHARD P, SUN Y et al. Nasopharyngeal carcinoma. Lancet 2019; 394: 64–80. https://doi.org/10.1016/S0140-6736(19)30956-0

[2] ZHOU J, GUO T, ZHOU L, BAO M, WANG L et al. The ferroptosis signature predicts the prognosis and immune microenvironment of nasopharyngeal carcinoma. Sci Rep 2023; 13: 1861. https://doi.org/10.1038/s41598-023-28897-2

[3] GUO Z, LI Z, ZHANG M, BAO M, HE B et al. LncRNA FAS-AS1 upregulated by its genetic variation rs6586163 promotes cell apoptosis in nasopharyngeal carcinoma through regulating mitochondria function and Fas splicing. Sci Rep 2023; 13: 8218. https://doi.org/10.1038/s41598-023-35502-z

[4] WEI K R, ZHENG RS, ZHANG SW, LIANG ZH, LI ZM et al. Nasopharyngeal carcinoma incidence and mortality in China, 2013. Chin J Cancer 2017; 36: 90. https://doi.org/10.1186/s40880-017-0257-9

[5] GUO Z, WANG YJ, HE BS, ZHOU J. Linc00312 Single Nucleotide Polymorphism as Biomarker for Chemoradiotherapy Induced Hematotoxicity in Nasopharyngeal Carcinoma Patients. Dis Markers 2022; 2022: 6707821. https://doi.org/10.1155/2022/6707821

[6] LIN X, YU T, ZHANG L, CHEN S, CHEN X et al. Silencing Op18/stathmin by RNA Interference Promotes the Sensitivity of Nasopharyngeal Carcinoma Cells to Taxol and High-Grade Differentiation of Xenografted Tumours in Nude Mice. Basic Clin Pharmacol Toxicol 2016; 119: 611–620. https://doi.org/10.1111/bcpt.12633

[7] YING K, LIU Y, ZHANG C, SHANGGUAN M. Medical findings of nasopharyngeal carcinoma patients and antitumor benefits of formononetin. Eur J Pharmacol 2019; 861: 172619. https://doi.org/10.1016/j.ejphar.2019.172619

[8] LIN JJ, FAN JJ, GE XJ, SHA HB. PAG1 stimulates proliferation and metastasis of nasopharyngeal carcinoma through downregulating PTEN. Eur Rev Med Pharmacol Sci 2020; 24: 11096–11104. https://doi.org/10.26355/eurrev_202011_23596

[9] LI Q G, XIAO T, ZHU W, YU ZZ, HUANG XP et al. HDAC7 promotes the oncogenicity of nasopharyngeal carcinoma cells by miR-4465-EphA2 signaling axis. Cell Death Dis 2020; 11: 322. https://doi.org/10.1038/s41419-020-2521-1

[10] SAINI VK, SEWAL RK, AHMAD Y, MEDHI B. Prospective Observational Study of Adverse Drug Reactions of Anticancer Drugs Used in Cancer Treatment in a Tertiary Care Hospital. Indian J Pharm Sci 2015; 77: 687–693. https://doi.org/10.4103/0250-474x.174990

[11] ZENG M, GUO D, FERNANDEZ-VARO G, ZHANG X, FU S et al. The Integration of Nanomedicine with Traditional Chinese Medicine: Drug Delivery of Natural Products and Other Opportunities. Mol Pharm 2023; 20: 886–904. https://doi.org/10.1021/acs.molpharmaceut.2c00882

[12] WANG Y, PENG F, XIE G, CHEN ZQ, LI HG et al. Rhubarb attenuates blood-brain barrier disruption via increased zonula occludens-1 expression in a rat model of intracerebral hemorrhage. Exp Ther Med 2016; 12: 250–256. https://doi.org/10.3892/etm.2016.3330

[13] ORLIKOVA B, LEGRAND N, PANNING J, DICATO M, DIEDERICH M. Anti-inflammatory and anticancer drugs from nature. Cancer Treat Res 2014; 159: 123–143. https://doi.org/10.1007/978-3-642-38007-5_8

[14] PENG W, CHEN L, LIU J. Celastrol inhibits gastric cancer cell proliferation, migration, and invasion via the FOXA1/CLDN4 axis. Toxicol Res (Camb) 2023; 12: 392–399. https://doi.org/10.1093/toxres/tfad024

[15] JAKUBIKOVA J, SEDLAK J. Garlic-derived organosulfides induce cytotoxicity, apoptosis, cell cycle arrest and oxidative stress in human colon carcinoma cell lines. Neoplasma 2006; 53: 191–199.

[16] GUO Y, LIU H, CHEN Y, YAN W. The effect of allicin on cell proliferation and apoptosis compared to blank control and cis-platinum in oral tongue squamous cell carcinoma. Onco Targets Ther 2020; 13: 13183–13189. https://doi.org/10.2147/OTT.S178718

[17] MIKAILI P, MAADIRAD S, MOLOUDIZARGARI M, AGHAJANSHAKERI S, SARAHROODI S. Therapeutic uses and pharmacological properties of garlic, shallot, and their biologically active compounds. Iran J Basic Med Sci 2013; 16: 1031–1048.

[18] CHAN JY, YUEN AC, CHAN RY, CHAN SW. A review of the cardiovascular benefits and antioxidant properties of allicin. Phytother Res 2013; 27: 637–646. https://doi.org/10.1002/ptr.4796

[19] KYUNG KH. Antimicrobial properties of allium species. Curr Opin Biotechnol 2012; 23: 142–147. https://doi.org/10.1016/j.copbio.2011.08.004

[20] CHU YL, HO CT, CHUNG JG, RAGHU R, LO YC et al. Allicin induces anti-human liver cancer cells through the p53 gene modulating apoptosis and autophagy. J Agric Food Chem 2013; 61: 9839–9848. https://doi.org/10.1021/jf403241s

[21] ZOU X, LIANG J, SUN J, HU X, LEI L et al. Allicin sensitizes hepatocellular cancer cells to anti-tumor activity of 5-fluorouracil through ROS-mediated mitochondrial pathway. J Pharmacol Sci 2016; 131: 233–240. https://doi.org/10.1016/j.jphs.2016.04.017

[22] ZHANG X, ZHU Y, DUAN W, FENG C, HE X. Allicin induces apoptosis of the MGC-803 human gastric carcinoma cell line through the p38 mitogen-activated protein kinase/caspase-3 signaling pathway. Mol Med Rep 2015; 11: 2755–2760. https://doi.org/10.3892/mmr.2014.3109

[23] XU L, YU J, ZHAI D, ZHANG D, SHEN W et al. Role of JNK Activation and Mitochondrial Bax Translocation in Allicin-Induced Apoptosis in Human Ovarian Cancer SKOV3 Cells. Evid Based Complement Alternat Med 2014; 2014: 378684. https://doi.org/10.1155/2014/378684

[24] TSUBURA A, LAI YC, KUWATA M, UEHARA N, YOSHIZAWA K. Anticancer effects of garlic and garlic-derived compounds for breast cancer control. Anticancer Agents Med Chem 2011; 11: 249–253. https://doi.org/10.2174/187152011795347441

[25] CHA JH, CHOI YJ, CHA SH, CHOI CH, CHO WH. Allicin inhibits cell growth and induces apoptosis in U87MG human glioblastoma cells through an ERK-dependent pathway. Oncol Rep 2012; 28: 41–48. https://doi.org/10.3892/or.2012.1772

[26] BAT-CHEN W, GOLAN T, PERI I, LUDMER Z, SCHWARTZ B. Allicin purified from fresh garlic cloves induces apoptosis in colon cancer cells via Nrf2. Nutr Cancer 2010; 62: 947–957. https://doi.org/10.1080/01635581.2010.509837

[27] TYAGI G, PRADHAN S, SRIVASTAVA T, MEHROTRA R. Nucleic acid binding properties of allicin: spectroscopic analysis and estimation of anti-tumor potential. Biochim Biophys Acta 2014; 1840: 350–356. https://doi.org/10.1016/j.bbagen.2013.09.007

[28] SONG B, SHU Y, CUI T, FU P. Allicin inhibits human renal clear cell carcinoma progression via suppressing HIF pathway. Int J Clin Exp Med 2015; 8: 20573–20580.

[29] WANG CJ, WANG C, HAN J, WANG YK, TANG L et al. Effect of combined treatment with recombinant interleukin-2 and allicin on pancreatic cancer. Mol Biol Rep 2013; 40: 6579–6585. https://doi.org/10.1007/s11033-013-2766-1

[30] BEDOUI S, HEROLD MJ, STRASSER A. Emerging connectivity of programmed cell death pathways and its physiological implications. Nat Rev Mol Cell Biol 2020; 21: 678–695. https://doi.org/10.1038/s41580-020-0270-8

[31] TANG D, KANG R, BERGHE TV, VANDENABEELE P, KROEMER G. The molecular machinery of regulated cell death. Cell Res 2019; 29: 347–364. https://doi.org/10.1038/s41422-019-0164-5

[32] BAYIR H, ANTHONYMUTHU TS, TYURINA YY, PATEL SJ, AMOSCATO AA et al. Achieving Life through Death: Redox Biology of Lipid Peroxidation in Ferroptosis. Cell Chem Biol 2020; 27: 387–408. https://doi.org/10.1016/j.chembiol.2020.03.014

[33] YANG WS, STOCKWELL BR. Ferroptosis: Death by Lipid Peroxidation. Trends Cell Biol 2016; 26: 165–176. https://doi.org/10.1016/j.tcb.2015.10.014

[34] FRIEDMANN ANGELI JP, KRYSKO DV, CONRAD M. Ferroptosis at the crossroads of cancer-acquired drug resistance and immune evasion. Nat Rev Cancer 2019; 19: 405–414. https://doi.org/10.1038/s41568-019-0149-1

[35] ELGENDY SM, ALYAMMAHI SK, ALHAMAD DW, ABDIN SM, OMAR HA. Ferroptosis: An emerging approach for targeting cancer stem cells and drug resistance. Crit Rev Oncol Hematol 2020; 155: 103095. https://doi.org/10.1016/j.critrevonc.2020.103095

[36] FORCINA GC, DIXON SJ. GPX4 at the Crossroads of Lipid Homeostasis and Ferroptosis. Proteomics 2019; 19: e1800311. https://doi.org/10.1002/pmic.201800311

[37] FRIEDMANN ANGELI JP, CONRAD M. Selenium and GPX4, a vital symbiosis. Free Radic Biol Med 2018; 127: 153–159. https://doi.org/10.1016/j.freeradbiomed.2018.03.001

[38] MAIORINO M, CONRAD M, URSINI F. GPx4, Lipid Peroxidation, and Cell Death: Discoveries, Rediscoveries, and Open Issues. Antioxid Redox Signal 2018; 29: 61–74. https://doi.org/10.1089/ars.2017.7115

[39] URSINI F, MAIORINO M. Lipid peroxidation and ferroptosis: The role of GSH and GPx4. Free Radic Biol Med 2020; 152: 175–185. https://doi.org/10.1016/j.freeradbiomed.2020.02.027

[40] STOCKWELL BR, JIANG X. The Chemistry and Biology of Ferroptosis. Cell Chem Biol 2020; 27: 365–375. https://doi.org/10.1016/j.chembiol.2020.03.013

[41] SU Y, ZHAO B, ZHOU L, ZHANG Z, SHEN Y et al. Ferroptosis, a novel pharmacological mechanism of anti-cancer drugs. Cancer Lett 2020; 483: 127–136. https://doi.org/10.1016/j.canlet.2020.02.015

[42] WANG H, CHENG Y, MAO C, LIU S, XIAO D et al. Emerging mechanisms and targeted therapy of ferroptosis in cancer. Mol Ther 2021; 29: 2185–2208. https://doi.org/10.1016/j.ymthe.2021.03.022

[43] SUN W, LIU DB, LI WW, ZHANG LL, LONG GX et al. Interleukin-6 promotes the migration and invasion of nasopharyngeal carcinoma cell lines and upregulates the expression of MMP-2 and MMP-9. Int J Oncol 2014; 44: 1551–1560. https://doi.org/10.3892/ijo.2014.2323

[44] LOU Z, GONG YQ, ZHOU X, HU GH. Low expression of miR-199 in hepatocellular carcinoma contributes to tumor cell hyper-proliferation by negatively suppressing XBP1. Oncol Lett 2018; 16: 6531–6539. https://doi.org/10.3892/ol.2018.9476

[45] WU W, LI H, WANG Z, DAI Z, LIANG X et al. The tertiary lymphoid structure-related signature identified PTGDS in regulating PD-L1 and promoting the proliferation and migration of glioblastoma. Heliyon 2024; 10: e23915. https://doi.org/10.1016/j.heliyon.2023.e23915

[46] SHEN F, LONG D, YU T, CHEN X, LIAO Y et al. Vinblastine differs from Taxol as it inhibits the malignant phenotypes of NSCLC cells by increasing the phosphorylation of Op18/stathmin. Oncol Rep 2017; 37: 2481–2489. https://doi.org/10.3892/or.2017.5469

[47] GAO Y, LIU Y, LIU Y, PENG Y, YUAN B et al. UHRF1 promotes androgen receptor-regulated CDC6 transcription and anti-androgen receptor drug resistance in prostate cancer through KDM4C-Mediated chromatin modifications. Cancer Lett 2021; 520: 172–183. https://doi.org/10.1016/j.canlet.2021.07.012

[48] LI M, XIAO Y, LIU M, NING Q, XIANG Z et al. MiR-26a-5p regulates proliferation, apoptosis, migration and invasion via inhibiting hydroxysteroid dehydrogenase like-2 in cervical cancer cell. BMC Cancer 2022; 22: 876. https://doi.org/10.1186/s12885-022-09970-x

[49] LI F, LI D, LIU H, CAO BB, JIANG F et al. RNF216 Regulates the Migration of Immortalized GnRH Neurons by Suppressing Beclin1-Mediated Autophagy. Front Endocrinol (Lausanne) 2019; 10: 12. https://doi.org/10.3389/fendo.2019.00012

[50] XIONG T, LI Z, HUANG X, LU K, XIE W et al. TO901317 inhibits the development of hepatocellular carcinoma by LXRalpha/Glut1 decreasing glycometabolism. Am J Physiol Gastrointest Liver Physiol 2019; 316: G598–G607. https://doi.org/10.1152/ajpgi.00061.2018

[51] WEI S, SUN T, DU J, ZHANG B, XIANG D et al. Xanthohumol, a prenylated flavonoid from Hops, exerts anticancer effects against gastric cancer in vitro. Oncol Rep 2018; 40: 3213–3222. https://doi.org/10.3892/or.2018.6723
[52] ZHAO Y, CHEN S, SHEN F, LONG D, YU T et al. In vitro neutralization of autocrine IL-10 affects Op18/stathmin signaling in non-small cell lung cancer cells. Oncol Rep 2019; 41: 501–511. https://doi.org/10.3892/or.2018.6795
[53] DRUMMEN GP, VAN LIEBERGEN LC, OP DEN KAMP JA, POST JA. C11-BODIPY (581/591), an oxidation-sensitive fluorescent lipid peroxidation probe: (micro)spectroscopic characterization and validation of methodology. Free Radic Biol Med 2002; 33: 473–490. https://doi.org/10.1016/s0891-5849(02)00848-1
[54] SPANGENBURG EE, PRATT SJP, WOHLERS LM, LOVERING RM. Use of BODIPY (493/503) to visualize intramuscular lipid droplets in skeletal muscle. J Biomed Biotechnol 2011; 2011: 598358. https://doi.org/10.1155/2011/598358
[55] LI D, SONG C, ZHANG J, ZHAO X. Resveratrol alleviated 5-FU-induced cardiotoxicity by attenuating GPX4 dependent ferroptosis. J Nutr Biochem 2023; 112: 109241. https://doi.org/10.1016/j.jnutbio.2022.109241
[56] SONG YX, LI X, NIE SD, HU ZX, ZHOU D et al. Extracellular vesicles released by glioma cells are decorated by Annexin A2 allowing for cellular uptake via heparan sulfate. Cancer Gene Ther 2023; 30: 1156–1166. https://doi.org/10.1038/s41417-023-00627-w
[57] SUN D, LI X, NIE S, LIU J, WANG S. Disorders of cancer metabolism: The therapeutic potential of cannabinoids. Biomed Pharmacother 2023; 157: 113993. https://doi.org/10.1016/j.biopha.2022.113993
[58] HE B, HOU F, REN C, BING P, XIAO X. A Review of Current In Silico Methods for Repositioning Drugs and Chemical Compounds. Front Oncol 2021; 11: 711225. https://doi.org/10.3389/fonc.2021.711225
[59] WEI Z, CHEN J, ZUO F, GUO J, SUN X et al. Traditional Chinese Medicine has great potential as candidate drugs for lung cancer: A review. J Ethnopharmacol 2023; 300: 115748. https://doi.org/10.1016/j.jep.2022.115748
[60] YANG Z, DU J, ZHU J, RONG Y, CHEN S et al. Allicin Inhibits Proliferation by Decreasing IL-6 and IFN-beta in HCMV-Infected Glioma Cells. Cancer Manag Res 2020; 12: 7305–7317. https://doi.org/10.2147/CMAR.S259677
[61] PANDEY N, TYAGI G, KAUR P, PRADHAN S, RAJAM MV et al. Allicin Overcomes Hypoxia Mediated Cisplatin Resistance in Lung Cancer Cells through ROS Mediated Cell Death Pathway and by Suppressing Hypoxia Inducible Factors. Cell Physiol Biochem 2020; 54: 748–766. https://doi.org/10.33594/000000253
[62] SCHULTZ CR, GRUHLKE MCH, SLUSARENKO AJ, BACHMANN AS. Allicin, a Potent New Ornithine Decarboxylase Inhibitor in Neuroblastoma Cells. J Nat Prod 2020; 83: 2518–2527. https://doi.org/10.1021/acs.jnatprod.0c00613
[63] CHEN H, ZHU B, ZHAO L, LIU Y, ZHAO F et al. Allicin Inhibits Proliferation and Invasion in Vitro and in Vivo via SHP-1-Mediated STAT3 Signaling in Cholangiocarcinoma. Cell Physiol Biochem 2018; 47: 641–653. https://doi.org/10.1159/000490019
[64] LI X, NI J, TANG Y, WANG X, TANG H et al. Allicin inhibits mouse colorectal tumorigenesis through suppressing the activation of STAT3 signaling pathway. Nat Prod Res 2019; 33: 2722–2725. https://doi.org/10.1080/14786419.2018.1465425
[65] LIU Y, ZHANG Y, TAN Z, WANG J, HU Y et al. Lysyl oxidase promotes anaplastic thyroid carcinoma cell proliferation and metastasis mediated via BMP1. Gland Surg 2022; 11: 245–257. https://doi.org/10.21037/gs-21-908
[66] WU Y, SUN W, KONG Y, LIU B, ZENG M et al. Restoration of microRNA-130b expression suppresses osteosarcoma cell malignant behavior in vitro. Oncol Lett 2018; 16: 97–104. https://doi.org/10.3892/ol.2018.8643
[67] ZHANG Q, YANG D. Allicin suppresses the migration and invasion in cervical cancer cells mainly by inhibiting NRF2. Exp Ther Med 2019; 17: 1523–1528. https://doi.org/10.3892/etm.2018.7104
[68] LV Q, XIA Q, LI J, WANG Z. Allicin suppresses growth and metastasis of gastric carcinoma: the key role of microRNA-383-5p-mediated inhibition of ERBB4 signaling. Biosci Biotechnol Biochem 2020; 84: 1997–2004. https://doi.org/10.1080/09168451.2020.1780903
[69] LI L, WANG S, ZHOU W. Balance Cell Apoptosis and Pyroptosis of Caspase-3-Activating Chemotherapy for Better Antitumor Therapy. Cancers (Basel) 2022; 15: 26. https://doi.org/10.3390/cancers15010026
[70] SUN L, WANG X. Effects of allicin on both telomerase activity and apoptosis in gastric cancer SGC-7901 cells. World J Gastroenterol 2003; 9: 1930–1934. https://doi.org/10.3748/wjg.v9.i9.1930
[71] ZHANG W, HA M, GONG Y, XU Y, DONG N et al. Allicin induces apoptosis in gastric cancer cells through activation of both extrinsic and intrinsic pathways. Oncol Rep 2010; 24: 1585–1592. https://doi.org/10.3892/or_00001021
[72] TAO M, GAO L, PAN J, WANG X. Study on the inhibitory effect of allicin on human gastric cancer cell line SGC-7901 and its mechanism. Afr J Tradit Complement Altern Med 2014; 11: 176–179. https://doi.org/10.4314/ajtcam.v11i1.28
[73] LI C, JING H, MA G, LIANG P. Allicin induces apoptosis through activation of both intrinsic and extrinsic pathways in glioma cells. Mol Med Rep 2018; 17: 5976–5981. https://doi.org/10.3892/mmr.2018.8552
[74] CHEN J, LI X, LIU H, ZHONG D, YIN K et al. Bone marrow stromal cell-derived exosomal circular RNA improves diabetic foot ulcer wound healing by activating the nuclear factor erythroid 2-related factor 2 pathway and inhibiting ferroptosis. Diabet Med 2023; 40: e15031. https://doi.org/10.1111/dme.15031
[75] SUN Z, ZOU X, BAO M, HUANG Z, LOU Y et al. Role of ferroptosis in fibrosis diseases. Am J Med Sci 2023; 366: 87–95. https://doi.org/10.1016/j.amjms.2023.04.024